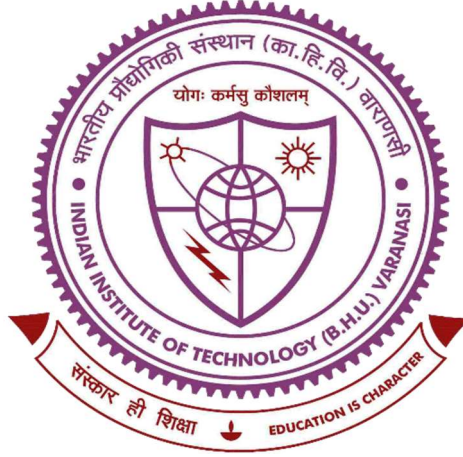


Development of Polymeric Nanomedicine for Accelerating Tissue Regeneration and Biological Activity Assessment of Antimicrobial Components



Thesis submitted in partial fulfilment
for the Award of Degree
Doctor of Philosophy

By

PREM SHANKAR GUPTA

SCHOOL OF BIOMEDICAL ENGINEERING
INDIAN INSTITUTE OF TECHNOLOGY
(BANARAS HINDU UNIVERSITY)
VARANASI-221005

Roll No. 17021505

2024



भारतीय
प्रौद्योगिकी
संस्थान
काशी हिन्दू विश्वविद्यालय



INDIAN
INSTITUTE OF
TECHNOLOGY
BANARAS HINDU UNIVERSITY

Dr. Pradip Paik, B.Tech. (C.U), M.Tech. & Ph.D. (IIT-K)
Associate Professor
School of Bio-Medical Engineering

Ref: Paik/IIT(BHU)/1

Varanasi, U.P., India

Phone.: +91-8500109932(m)

Fax: +91-..-

Email: paik.bme@iitbhu.ac.in,
pradip.paik@gmail.com

Date: 29th January, 2024

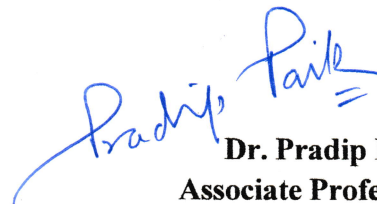
CERTIFICATE

This is to certify that the dissertation entitled, "**Development of Polymeric Nanomedicine for Accelerating Tissue Regeneration and Biological Activity Assessment of Antimicrobial Components**" submitted by Mr. **Prem Shankar Gupta** (Reg. No. **17021505**) in partial fulfilment of the requirements for the award of Doctor of Philosophy (Ph.D.) in the School of Biomedical Engineering, Indian Institute of Technology, BHU, Varanasi, India, is a bona fide record of research work carried out by him under my supervision and guidance.

This dissertation is free from plagiarism (report attached) and has not been submitted previously in part or in full to this or any other university or institution for the award of any degree or diploma. It is also certified that the student has fulfilled all the requirements to submit this dissertation.

Further, parts of this dissertation have been filed for patents or published in peer-reviewed journals to fulfil the requirement of the Degree and all rights reserve to the Institute (IIT BHU).

Dr. Pradip Paik, Ph.D.
Associate Professor
School of Biomedical Engineering
Indian Institute of Technology (BHU)
Varanasi 221 005, U.P., India


Dr. Pradip Paik,
Associate Professor,
School of Biomedical Engineering
Indian Institute of Technology, BHU
Varanasi

IIT - BHU



SCHOOL OF BIOMEDICAL ENGINEERING
INDIAN INSTITUTE OF TECHNOLOGY (BHU)
paik.bme@iitbhu.ac.in, pradip.paik@gmail.com
<http://www.iitbhu.ac.in/bme>



भारतीय
प्रौद्योगिकी
संस्थान
काशी हिन्दू विश्वविद्यालय



INDIAN
INSTITUTE OF
TECHNOLOGY
BANARAS HINDU UNIVERSITY

Dr. Pradip Paik, B.Tech. (C.U), M.Tech. & Ph.D. (IIT-K)
Associate Professor
School of Bio-Medical Engineering

Ref: Paik/IIT(BHU)/1

Varanasi, U.P., India

Phone.: +91-8500109932(m)

Fax: +91-..-

Email: paik.bme@iitbhu.ac.in,
pradip.paik@gmail.com

Date: 29th January, 2024

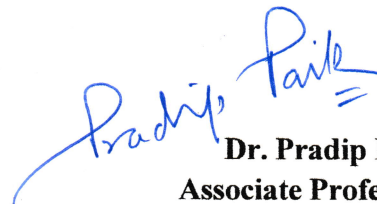
CERTIFICATE

This is to certify that the dissertation entitled, "**Development of Polymeric Nanomedicine for Accelerating Tissue Regeneration and Biological Activity Assessment of Antimicrobial Components**" submitted by Mr. **Prem Shankar Gupta** (Reg. No. **17021505**) in partial fulfilment of the requirements for the award of Doctor of Philosophy (Ph.D.) in the School of Biomedical Engineering, Indian Institute of Technology, BHU, Varanasi, India, is a bona fide record of research work carried out by him under my supervision and guidance.

This dissertation is free from plagiarism (report attached) and has not been submitted previously in part or in full to this or any other university or institution for the award of any degree or diploma. It is also certified that the student has fulfilled all the requirements to submit this dissertation.

Further, parts of this dissertation have been filed for patents or published in peer-reviewed journals to fulfil the requirement of the Degree and all rights reserve to the Institute (IIT BHU).

Dr. Pradip Paik, Ph.D.
Associate Professor
School of Biomedical Engineering
Indian Institute of Technology (BHU)
Varanasi 221 005, U.P., India


Dr. Pradip Paik,
Associate Professor,
School of Biomedical Engineering
Indian Institute of Technology, BHU
Varanasi

IIT - BHU



SCHOOL OF BIOMEDICAL ENGINEERING
INDIAN INSTITUTE OF TECHNOLOGY (BHU)
paik.bme@iitbhu.ac.in, pradip.paik@gmail.com
<http://www.iitbhu.ac.in/bme>

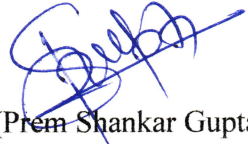
DECLARATION BY THE CANDIDATE

I, "PREM SHANKAR GUPTA" (Reg. No. 17021505) certify that the work embodied in this dissertation: "Development of Polymeric Nanomedicine for Accelerating Tissue Regeneration and Biological Activity Assessment of Antimicrobial Components", is my own bona fide work and carried out by me under the supervision of DR. PRADIP PAIK, School of Biomedical Engineering, Indian Institute of Technology, BHU, Varanasi, India, from "2017" to "2024", at the School of Biomedical Engineering, Indian Institute of Technology (BHU), Varanasi, India.

I declare that I have faithfully acknowledged the research works and have been cited them whichever have been followed to carry out the work of this Dissertation.

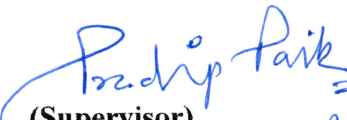
This dissertation is free from plagiarism and has not been submitted previously in part or in full to this or any other university or institution for the award of any degree or diploma.


Place: IIT BHU
Date: 29. January, 2024


(Prem Shankar Gupta)

CERTIFICATE BY THE SUPERVISOR

It is certified that the statement made by student is true to the best our knowledge.


(Supervisor)
Dr. Pradip Paik,
Associate Professor,
School of Biomedical Engineering,
Indian Institute of Technology, BHU, Varanasi, India
29/01/2024


(COORDINATOR)
29.01.24
School of Biomedical Engineering,
Indian Institute of Technology, BHU, Varanasi
समन्वयक/CO-ORDINATOR
जैव चिकित्सा अभियांत्रिकी स्कूल
SCHOOL OF BIOMEDICAL ENGG.
भारतीय प्रौद्योगिकी संस्थान (का.हि.वि.)
INDIAN INSTITUTE OF TECHNOLOGY (B.H.U.)
वाराणसी-221005/VARANASI-221005

COPY RIGHT TRANSFER CERTIFICATE

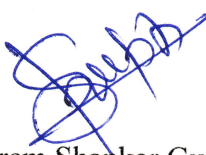
Title of thesis: **“Development of Polymeric Nanomedicine for Accelerating Tissue Regeneration and Biological Activity Assessment of Antimicrobial Components”.**

Candidate's Name: Prem Shankar Gupta

Copyright Transfer

The undersigned hereby assigns to the Indian Institute of Technology (Banaras Hindu University), Varanasi - 21005, India, all right under the copyright that may exist in and for the above thesis submitted for the award of the doctor of philosophy.

Date: 29/01/2024
Place: IIT (BHU), Varanasi


(Prem Shankar Gupta)

Note: However, the author may reproduce or authorize others to reproduce material extracted verbatim from the thesis, or derivative of the thesis for the author's personal use, provided that the source and the institute's copyright notice are indicated.

Acknowledgement

This is my chance to sincerely thank everyone who has helped and advised me on my research path. I owe a great deal of gratitude to the several people who have provided crucial support and encouragement in shaping my thesis to its current state.

I want to start by sincerely thanking Dr. Pradip Paik, my supervisor, for giving me this study opportunity. This effort has been completed in large part because to his constant inspiration, support, and advice. I also owe a debt of gratitude to Dr. Sanjeev Mahto and Ashutosh Dubey, who served on my research progress evaluation committee and whose insightful advice, insightful remarks, and unwavering encouragement greatly improved the quality of my work.


I would like to express my gratitude to Professor Neeraj Sharma, Professor Prasun K. Roy, Dr. Sanjay K. Rai, Dr. Shiru Sharma, Dr. AR Jac Frado, Dr. Sudeep Mukharjee, Dr. Deepesh, Dr. Brijesh, and Dr. Gauri of the School for their invaluable assistance in facilitating all official, motivational procedures, and paperwork. I am appreciative of the school's supporting personnel for their helpful assistance whenever required.

I would like to express my heartfelt gratitude to Prof. Rajeev Prakash and the CIFIC personnel for their unwavering support and assistance throughout the research process. I am grateful to have friends such as Dr. Soniya Rani, Pankaj Jain, Kirti, Divya, Sukanya, Gurmeet, DD, Nillmani, Sumit, Bindu, Snehlata, Prateek, Richa, and Parul who have always supported me in difficult times.

Lastly, I would want to convey my profound appreciation to my family for their steadfast affection, support, and confidence. I would want to express my sincere gratitude to my parents and my in-laws for their unwavering support in all of my endeavours. I would want to express my sincere gratitude to my wife, Prof. (Dr.) Namita Gupta, for her unwavering love and support during this endeavour; she is a consistent source of motivation for me. I am very thankful for the enormous love and patience that my daughter and son have given me.

Appreciation is extended to everyone.

Date..... 29/01/2024
Place..... IIT (BHU), Varanasi


Prem Shankar Gupta

List of Figures

Figure 1.1:	Worldwide wound statistics (in millions)1
Figure 1.2:	Wound healing phases – Wound healing unfolds through distinct phases: Haemostasis, inflammation, proliferation and migration, and remodelling. Commencing immediately, the first phase involves blood clotting, while the second phase focuses on wound cleansing, marked by immune cell infiltration and activation. Days later, the third phase sees cell proliferation, migration, and differentiation, particularly in epithelial, endothelial, and fibroblast cells reconstructing new tissue. The concluding maturation phase, lasting weeks to months, entails the strengthening and remodelling of the newly formed tissue.....6
Figure 1.3:	Biomaterials based nanotherapeutics exerts their regenerating effect at different stages of wound healing.....10
Figure 1.4:	The biological attributes of nitric oxide (NO) play pivotal roles in vasodilation, blood clotting, neurotransmission, apoptosis, angiogenesis, re-epithelization, collagen synthesis, and antimicrobial functions. Notably, among these biological characteristics, the angiogenic activity, re-epithelization, and collagen synthesis prove beneficial in facilitating the wound healing process.....29
Figure 2.1	Apparatus for measurement of the spreadability of nanoformulation..72
Figure 2.2:	Content uniformity test. SP nanoformulation filled syringe tubes, tube was cut into pieces and content was evaluated for uniformity.....74
Figure 2.3:	<i>In vitro</i> dissolution of SP nanoformulation.....75
Figure 3.1.1:	Prepared PNAG NPs are formulated into nanoformulation, and applied on rats' wounds. Accelerated wound healing was observed due to a reduction in inflammation and induction of cell migration, proliferation and angiogenesis.....85
Figure 3.1.2:	Synthesis mechanism of N-Acryloyl Glycine (NAG) monomer.....91
Figure 3.1.3:	FTIR spectra and XRD pattern of NAG monomer and PNAG NPs. FTIR spectra show the absorption bands for (a) NAG monomer and (b) PNAG polymer; the XRD pattern (c) shows that NAG monomer is highly crystalline, while (d) the synthesised PNAG NPs show reduced crystallinity compared to the NAG monomer.....91
Figure 3.1.4:	¹ H-NMR spectrum of N-acryloyl-glycine (NAG), monomer recorded in DMSO deuterated (500 MHz).....92

Figure 3.1.5:	¹³ C-NMR spectrum of N-acryloyl-glycine (NAG), monomer recorded in DMSO deuterated (500 MHz).....	93
Figure 3.1.6:	¹ H-NMR spectrum of Poly-N-acryloyl-glycine (PNAG), monomer recorded in CDCl ₃ deuterated (500 MHz).....	93
Figure 3.1.7:	¹³ C-NMR spectrum of Poly-N-acryloyl-glycine (PNAG), monomer recorded in CDCl ₃ deuterated (500 MHz).....	94
Figure 3.1.8:	TEM micrograph and particle size distribution of PNAG NPs; (a) reveal net-like co-connect arrangements; (b) particle size distribution of PNAG NPs calculated considering 300 particles; (c) shows porous particle structure and (d) SAED pattern shows diffused rings and confirms semi-crystalline nature of PNAG NPs.....	94
Figure 3.1.9:	PNAG NPs particle size recorded by dispersing in PBS (pH 7.4).....	95
Figure 3.1.10:	PNAG NPs zeta potential recorded by dispersing in PBS (pH 7.4).....	96
Figure 3.1.11:	Cytotoxicity and hemocompatibility of PNAG NPs. (a) Cytotoxicity of the NAG monomer and PNAG NPs in the L929 cell line and (b) PNAG NPs in HUVEC cells. (c) and (d) Effect of different concentrations of PNAG NPs on the blood coagulation cascade in terms of PT (c) and APTT (d). The zones between the black dashed lines represent reference values for PT and APTT. Both the coagulation pathways (PT and APTT) were tested separately. (e) Dose–response curve for the haemolytic activity of PNAG NPs in rat erythrocytes, showing no significant difference (p > 0.05); (f) haemolysis (%) compared to the control caused by 0.1% dispersion of PNAG NPs and 0.1% Triton X-100 solution in PBS (p > 0.05); the outcomes represent the mean ±SD of three separate studies.....	98
Figure 3.1.12:	<i>In vitro</i> scratch wound healing assay; (a) microscopic assay images obtained at 0, 24 and 48 h. Images were captured at 10X magnification, and the scale bars indicate 100 μm. Assay was conducted using PNAG NPs in a concentration and time-dependent manner. Treatment: Control (complete cell culture media) and PNAG50, 100 and 200 (PNAG NPs in complete cell culture media at a concentration of 50, 100 and 200 μg. mL ⁻¹); (b) L929 cells showing <i>in vitro</i> wound closure (%) and (c) rate wound closure (%). Data are given as mean, standard deviation (n = 3), (*P < 0.05, ***P < 0.001).....	101
Figure 3.1.13:	Angiogenic assay: Angiogenic effect of PNAG NPs in chicken embryo membrane Assay (CEMA). (a) PNAG NPs stimulate vessels sprouting in the CAM model compared to the reference. Histogram shows the increase in vascular density (b), vascular length density (c) and mean development area (d) as a function of time for a specified vessel structure compared with the reference. The values presented are the	

- mean \pm SD of three independent experiments. * $p < 0.05$ is considered significant when compared to normal ($n=3$).....103
- Figure 3.1.14: *In vivo* skin irritation study in Wistar rats. (A) Results show the dermal irritation study in Wistar rats after dermal application. Images were taken before (0 h) and after (24h) application of samples; (a, b) Positive control (1% formalin solⁿ), (c, d) control (formulation base), (e, f) treatment (PNAG-nanoformulation), respectively. After 24 h of application, control group (d) and treatment group (f) does not show any sign and symptoms of dermal toxicity, i.e., dermal irritancy, while in the positive control group (b) showed significant erythema and oedema at the site of application (in red circle).....106
- Figure 3.1.15: *In vivo* wound healing study conducted in Wistar rats. Photo images of wound healing after 0, 1, 3, 7, 9, 11, 13 and 14 days; in Wistar rats treated with formulation base (control) and PNAG nanoformulation (treatment group).....108
- Figure 3.1.16: *In vivo* wound healing study conducted in Wistar rats. Wound closure profiles of animals treated with formulation base (control group) and PNAG nanoformulation (treatment group) ($p < 0.05$). Data are presented as the mean \pm standard deviation ($n=3$).....109
- Figure 3.1.17: Histological evaluation on day 14th post-wounding involved a comparison with healthy skin tissue (a), control tissue (base nanoformulation) (b), and PNAG nanoformulation (c). Images at 4x, 10x, and 40x magnifications (denoted by numbers 1, 2, and 3). Healthy skin images (a1, a2 and a3) exhibited well-defined structures such as dead skin, epithelium, collagen fibre-rich dermis, hypodermis, smooth muscle fibre, sweat gland, sebaceous gland, hair follicle, blood vessels, nerve endings, papillary dermis, and reticular dermis rete ridges. Control skin images (b1, b2 and b3) displayed compromised healing, evidenced by broken epithelium, underdeveloped dermis fibres, the absence of hypodermis, undifferentiated reticular dermis, and no rete ridges of the epidermis. While, PNAG nanoformulation-treated skin images (c1, c2 and c3) showcased a well-differentiated epidermis, underdeveloped basal layer, fully differentiated and grown blood vessels, thickened epidermis layers in some areas, fully developed epidermal ridges, mature granuloma, phases of remodelling, and a meshy structure in the papillary dermis and reticular dermis, with the presence of large fibres.....111
- Figure 3.1.18: Immunochemical analysis: (a) TNF- α , (b) IL-6, and (c) IGF. PNAG NPs enhance the concentration and levels of IGF-1 (c) and regulate pro-inflammatory cytokines and chemokines TNF- α (a) and IL-6 (b)....113
- Figure 3.2.1: Prepared PNAG NPs loaded with sodium nitroprusside (SNP a nitric oxide gas-releasing molecule) induce cell migration, proliferation, and

	angiogenesis, reducing inflammation and accelerating <i>in vivo</i> wound healing.....	127
Figure 3.2.2:	Ninhydrin test. (a) Glycine amino acid gives vibrant blue/ violet colour, (b and c) NAG monomer and PNAG NPs does not respond to ninhydrin test, showing absence of free amino group (-NH ₂).....	133
Figure 3.2.3:	Characterisation of SP NPs. FTIR spectra of (a) PNAG NPs, (b) Sodium nitroprusside (SNP) and (c) SP NPs. XRD pattern of (d) PNAG NPs, (e) SNP and (f) SP NPs. TEM images of SP NPs (g, h and i), SAED pattern (j), and particle sizes (k) were calculated from TEM images (number of particles > 400) and DLS (l).....	134
Figure 3.2.4:	SEM Images and Elemental Mapping Images of PNAG NPs (a1-g1) and SP NPs (a2-g2). Elements overlay for PNAG NPs, 92.9 (b1), 2.04 (c1), 4.84 (d1), 0.0 (e1), 0.21 (g1), and for SP NPs, 79.12 (b2), 1.38 (c2), 1.26 (d2), 7.66 (e2), and 10.59 (f2) %, respectively of C, N, O, Na and Fe. Mapping of C elements (b1, b2), Mapping of N elements (c1, c2), Mapping of O elements (d1, d2), Mapping of Na elements (e1, e2) and Mapping of Fe element (f1, f2) and merged of all element mapping (g1, g2), in the sample of PNAG NPs and SP NPs, respectively.....	135
Figure 3.2.5:	<i>In vitro</i> NO release profile. (a) Cumulative NO release profile (% CDR). (b) real-time NO release determination. NO release study was conducted from SP NPs in PBS (pH 7.4) at 37 °C. Data presented as mean ± SD (n=3).....	138
Figure 3.2.6:	Cytocompatibility and Hemocompatibility of SP NPs. (a) Cytocompatibility assay: treatment of mouse fibroblast (L929) cells with SP NPs shows proliferation instead of cytotoxicity. (P<0.05). (b) Activated partial thromboplastin time (APTT) and (c) Prothrombin time (PT) tested using different concentrations of SP NPs in the range of 1-200 µg mL ⁻¹ and compared to the control group (PBS-treated group). (p> 0.05). Data are presented as mean ±SD (n = 3). Haemolytic effect of SP NPs (d and e) on rat RBCs. (d) dose-response curves of haemolysis caused by SP NPs with concentrations ranging from 1 to 1000 µg mL ⁻¹ (p>0.05). (e) SP NPs show less than 1% haemolytic activity, even at the highest tested concentration (1000 µg mL ⁻¹), and haemolysis occurred in rat RBCs by SP NPs dispersion (0.1% w/v in PBS) compared with triton-X100 (0.1% v/v, positive control) against rat erythrocytes. Positive control shows ~15% haemolysis, while SP NPs show ~0.57% (p<0.05).....	139
Figure 3.2.7:	Scratch wound assay. (a) microscopic images of scratch wounds created in mouse fibroblast (L929) cells after being treated with SP NPs at concentrations of 50 µg mL ⁻¹ , 100 µg mL ⁻¹ , and 200 µg mL ⁻¹ compared to control at 0, 24, and 48 h. Images were acquired at 10x magnification, and the scale bar shows 100µm. (b) The time taken for cells to fill a 50% scratch gap determines how quickly cells migrated towards the scratch gap. (c) Remaining scratch area to be covered by cells.....	143

- Figure 3.2.8: Live/ dead assay: Figures displaying illustrations of live and dead L929 cells, after day-1 (a) and day-3 (b) of treatment with control, PNAG at $100 \mu\text{g mL}^{-1}$, SP NPs at 50, 100, 200 $\mu\text{g mL}^{-1}$. Scale bar = 100 μm . Cells were stained with Acridine orange and Propidium iodide.....144
- Figure 3.2.9: *In vivo* Chick Embryo Angiogenesis Assay (CEMA): (a) Determination of the effect of SP NPs on the formation and development of blood vessels in chick embryo model. Corresponding quantitative assessment of vascular development: (b) explant area, (c) vessels area, (d) total number of junctions, (e) vessel length, (f) average vessel length, and (g) total number of endpoints.....147
- Figure 3.2.10: NO release profile of SP nanoformulation (PBS, pH 6.8, 37°C, n=3). (a) Cumulative drug release, 79.35 \pm 4.43% NO was released from SP nanoformulation within 24h, showing controlled and sustained release, (b) Real-time NO release profile.....147
- Figure 3.2.11: Photographs of skin irritation study. Positive control (a1) before treatment, (a2) application of 1% formalin solution, (a3) erythema and oedema (shown in red circle) after 24h of application of 1% standard solution, (b1, b2 and b3) control (formulation base) treatment group and (c1, c2 and c3) treatment (SP nanoformulation) group not showing any skin sensitivity and irritation after 24 h of treatment of the respective samples.....150
- Figure 3.2.12: *In vivo* wound healing assessment: (a) Macroscopic images of wounds. (b) Measurement of relative wound area remaining to heal. (c) Range of wound size at 11th day that remained to heal. (d) Significant difference representation of mean wound size on the 11th day using the Tukey test to compare the mean. (e) Time-line of *in vivo* animal experimentation.....152
- Figure 3.2.13: Histological analysis of skin wound through staining with H & E stain and Mallory's trichrome stain. Histological assessment and comparative histological analysis of wound at post-injury with normal tissue stained with H & E (A, B and C) respectively at 2nd, 7th and 14th day and with Mallory's trichrome stain at 14th day (D) and comparative evaluation on 2nd, 7th and 14th day (E). Letter N, C and T denotes the images of healthy skin, control group (ointment base treated group) and treatment group (SP nanoformulation treated group), respectively. Image A, B, C and D at 100X and E at 20X.....154
- Figure 3.2.14: sqRT-PCR outcomes. (a) Relative expression of various genes during wound healing. (b) and (c) represent the gene expression level relative to GAPDH (in folds) for control and treatment group respectively for VEGFA, PECAM-1 and KDR. In figure, band of gene expression for the day 2 (C-2), day 7 (C-7) and day 14 (C-14) for control group and for the day 2 (T-2), day 7 (T-7) and day 14 (T-14) for the treatment group.....158

Figure 3.2.15:	Wound healing markers analysis by ELISA on the 2 nd , 7 th and 12 th days of post-wounding. (a) TNF- α , (b) IL-1 β , (c) IL-6, (d) CRP and (e) IGF-1 levels. Each data point represents the average (\pm SD) of 3 independent determinations ($p < 0.05$).....	161
Figure 3.3.1:	Illustrative image showing the metal oxide nanoparticles penetrating the deep tissue, interacting with microbes, creating a protective aura in the wound microenvironment and supporting the vascular system....	174
Figure 3.3.2:	HR-TEM image of: (a) ZnO, (b) ZnO-CuO (c) ZnO-Ag ₂ O/Ag, (d) ZnO-SnO ₂ NPs; SAED pattern for (e) ZnO, (f) ZnO-CuO, (g) ZnO-Ag ₂ O/Ag (h) ZnO-SnO ₂ NPs and d-spacing for (i) ZnO, (j) ZnO-CuO, (k) ZnO-Ag ₂ O/Ag, (l) ZnO-SnO ₂	179
Figure 3.3.3:	X-Ray diffraction pattern of (a) ZnO (b) ZnO-CuO (c) ZnO-SnO ₂ and (d) ZnO-Ag ₂ O/Ag NPs.....	179
Figure 3.3.4:	BET surface area of (a) ZnO, (b) ZnO-SnO ₂ (c) ZnO-CuO and (d) ZnO-Ag ₂ O/Ag NPs.....	180
Figure 3.3.5:	Antibacterial activity evaluation of (a) ZnO, (b) ZnO-SnO ₂ , (c) ZnO-CuO, (d) ZnO-Ag ₂ O/Ag NPs at different time interval with <i>E. coli</i> ...	183
Figure 3.3.6:	Haemolytic outcomes observed when rat RBCs treated with ZnO NPs.....	185
Figure 3.3.7:	Haemolytic outcomes of ZnO-Ag ₂ O/Ag NPs when evaluated in rat RBCs at 37 \pm 2 $^{\circ}$ C.....	185
Figure 3.3.8:	Haemolysis results of ZnO-CuO NPs interactions with rat RBCs.....	186
Figure 3.3.9:	Haemolytic outcomes of ZnO-SnO ₂ NPs in rat RBCs.....	187
Figure 3.3.10:	Comparative haemolytic activity of metal oxide NPs interacted with rat RBCs for 24 hours and 37 $^{\circ}$ C.....	187
Figure 3.3.11:	MTT assay of metal oxides in L929 cells. (a) ZnO, (b) ZnO-Ag ₂ O/Ag, (c) ZnO-CuO and ZnO-SnO ₂	189
Figure 3.3.12:	Cytocompatibility evaluation of metal oxide NPs in PC12 cell line. (a) ZnO, (b) ZnO-CuO, (c) ZnO-Ag ₂ O/Ag and (d) ZnO-SnO ₂ are incubated in the concentrations range of 1-250 μ g mL ⁻¹ with PC12 cell line.....	189
Figure 3.3.13:	Scratch wound assay conducted on L929 cell line at different concentration of ZnO and ZnO-CuO.....	191
Figure 3.3.14:	Scratch wound assay conducted on L929 cell line at different concentration of ZnO-SnO ₂ and ZnO-Ag ₂ O/Ag.....	192

Figure 3.3.15:	Scratch wound assay conducted in L929 cell lines by incubating metal oxides for 48 h. (a) ZnO, (b) ZnO-SnO ₂ , (c) ZnO-CuO and (d) ZnO-Ag ₂ O/Ag.....	193
Figure 3.3.16:	Angiogenic effect of ZnO NPs. (a) Photographic images of CAM at different time points, assessment of angiogenic parameter (b) explant area and (c) vessels area.....	196
Figure 3.3. 17:	Angiogenic effect of ZnO-Ag ₂ O/Ag NPs. (a) Photographic images of CAM at different time points, assessment of angiogenic parameter (b) explant area and (c) vessels area.....	197
Figure 3.3.18:	Angiogenic effect of ZnO-CuO NPs. (a) Photographic images of CAM at different time points, assessment of angiogenic parameter (b) explant area and (c) vessels area.....	198
Figure 3.3. 19:	Angiogenic effect of ZnO-SnO ₂ NPs. (a) Photographic images of CAM at different time points, assessment of angiogenic parameter (b) explant area and (c) vessels area.....	199

List of Tables

Table 1.1:	Polymers used in wound healing.....	15
Table 1.2:	Inorganic nanomaterials used in wound healing.....	19
Table 1.3:	Various gases used as wound healing therapeutics and their respective mechanism.....	28
Table 2.1:	The following materials were used during the execution of this project work.....	60
Table 2.2:	Table showing the ingredients (in percentage) used for the preparation of oleaginous ointment base.....	73
Table 2.3:	Dermal irritability grading system according to Draize.....	78
Table 3.1.1:	Qualitative characterization of base formulation and PNAG-nanoformulation on the basis of observational parameters.....	105
Table 3.1.2:	<i>In vivo</i> wound healing results shown in terms of relative area of wound.....	108
Table 3.2.1:	Elemental mapping results of PNAG NPs and SP NPs showing in weight percentage and atom percentage.....	137
Table 3.2.2:	Qualitative evaluation of SP Nanoformulation.....	148
Table 3.3.1:	Samples and Corresponding BET Surface Areas.....	182
Table 3.3.2:	Average scratch cover area (%) by L929 cell lines after incubation with metal oxide NPs at different concentrations for 48 h.....	194
Table 3.3.3:	Angiogenic outcome of ZnO NPs.....	195
Table 3.3.4:	Angiogenic outcome of ZnO-Ag ₂ O/Ag NPs.....	197
Table 3.3.5:	Angiogenic outcome of ZnO-CuO NPs.....	198
Table 3.3.6:	Angiogenic outcome of ZnO-SnO ₂ NPs.....	199

List of Abbreviations

Ag ₂ O/Ag NPs or Ag NPs	Silver Nanoparticles
AIBN	A, A'-Azoisobutyronitrile
ANOVA	Analysis Of Variance
AO	Acridine Orange
APTT	Activated Partial Thromboplastin Time
Ar	Argon
ATP	Adenosine Triphosphate
Au NPs	Gold Nanoparticles
BET analysis	Brunauer–Emmett–Teller Analysis
BG	Bioactive Glasses
CAM assay or CEMA	Chicken Embryo Angiogenesis Assay
CDR (%) or %CDR	Cumulative Drug Release
CeO ₂ NPs	Cerium Oxide Nanoparticles
CNT	Carbon Nanotube
CO	Carbon Monoxide
CO ₂	Carbon Dioxide
CRP	C-Reactive Protein
CuO NPs or Cu NPs	Copper Nanoparticles
DA	Developmental Area
DAMP	Damage-Associated Molecular Patterns
DEPC treated water	Diethyl Pyrocarbonate Treated Water
DFU	Diabetic Foot Ulcers
DLS	Dynamic Light Scattering
DMEM	Dulbecco's Modified Eagle Medium Culture Media
DMSO	Dimethyl Sulfoxide
DNA	Deoxyribonucleic Acid
DVB	Divinylbenzene
ECM	Extracellular Matrix
EDTA	Ethylenediaminetetraacetic Acid
EE%	Entrapment Efficiency
EGF	Epidermal Growth Factor
ELISA	Enzyme-Linked Immunosorbent Assay
eNOS	Endothelial Nitric Oxide Synthase
FBS	Fetal Bovine Serum
Fe NPs	Iron Nanoparticles
FTIR	Fourier-Transform Infrared Spectroscopy
GO	Graphene Oxide
GO NPs	Graphene Oxide Nanoparticles
GTP	Guanosine 5-Triphosphate
H&E	Haematoxylin And Ethyl Eosin
H ₂	Molecular Hydrogen
HBOT	Hyperbaric Oxygen Therapy
HD	Hexadecane
HDPs	Host Defence Peptides
He	Helium
HUVEC	Human Umbilical Vein Endothelial Cells

IGF-1	Insulin-Like Growth Factor 1
IL-10	Interleukin 10
IL-1 β	Interleukin 1 <i>Beta</i>
IL-6	Interleukin 6
IL-8	Interleukin 8
KBr	Potassium Bromide
KOH	Potassium Hydroxide
LC%	Loading Capacity
M1	Pro-Inflammatory Macrophage
M2	Anti-Inflammatory Macrophage
MCP-1	Monocyte Chemoattractant Protein-1
MMPs	Matrix Metalloproteinase
MONPs	Metal oxide nanoparticles
MOs	Metal Oxide/ Metal Oxides
MTT	3-(4,5-Dimethyl-2-Thiazolyl)-2,5-Diphenyl-2H-Tetrazolium Bromide
NAG	N-Acryloyl Glycine
NLCs	Nanostructured Lipid Carriers
NMR	Nuclear Magnetic Resonance Spectroscopy
NO	Nitric Oxide
NORM	Nitric Oxide Releasing Molecules
NP/ NPs	Nanoparticle/Nanoparticles
NWCC	National Wound Care Center
O ₂	Oxygen
O ₃	Ozone
PAMPs	Pathogen-Associated Modifying Proteins
PBS	Phosphate-Buffered Saline
PCL	Polycaprolactone
PDII	Primary Dermal Irritation Index
PEG	Polyethylene Glycol
PEO	Polyethylene Oxide
PI	Propidium Iodide
PLA	Poly(lactic Acid)
PLGA	Poly-Lactic-Co-Glycolic Acid
PNAG	Poly(N-Acryloyl Glycine)
PNAG NPs	Poly(N-Acryloyl Glycine) Nanoparticles
PT	Prothrombin Time
PU	Polyurethane
PVA	Polyvinyl Alcohol
RBCs	Erythrocytes Or Red Blood Cells
RNA	Ribonucleic Acid
ROS	Reactive Oxygen Species
RPM	Revolutions Per Minute
SD	Standard Deviation
SDS	Sodium Dodecyl Sulfate
SEM	Scanning Electron Microscopy
sGC	Soluble Guanylate Cyclase
Si NPs	Silicon Oxide/ Silica Nanoparticles
SLN	Solid Lipid Nanoparticles

SnO ₂ NPs	Tin Nanoparticles
SNP	Sodium Nitroprusside
SO ₂	Sulphur Dioxide
SP NPs	Nitric Oxide Releasing Nanoparticles/ Sodium Nitroprusside Loaded PNAG Nps
sqRT-PCR	Semi-Quantitative Reverse Transcription and Polymerase Chain Reaction
TE	Tissue Engineering
TEM or HRTEM	High-Resolution Transmission Electron Microscopy
TGF-β	Transforming Growth Factor-Beta
TiO ₂ NPs	Titanium Oxide Nanoparticles
TMB	Tetramethyl Benzidine
TNFα	Tumour Necrosis Factor Alpha
USD	United States Dollars
USP	United States Pharmacopoeia
UV	Ultra Violet Light/ Rays
UV-Vis	Ultraviolet-Visible
VDM	Vascular Density Measurement
VEGF	Vascular Endothelial Growth Factor
VLDM	Vasculature Length Density Measurement
WH	Wound Healing
WHO	World Health Organization
XRD	X-Ray Diffraction Analysis
ZnO NPs	Zinc Oxide Nanoparticles

Preface

The nexus of biopolymers, nanomedicine, and tissue engineering invites us to enter a world where the urgency of healing and the artistic quality of study collide in the always changing field of science. The pages that follow describe a story of creativity, accuracy, and the unwavering research for answers in the fields of wound healing and regenerative nanomedicine as we set out on our intellectual research journey.

Chapter 1: Introduction and background

We begin by delving into the complexities of biopolymers and investigating the exciting field of polymer nanoparticles, nanocapsules, and nanomedicines. Uncovering the many uses of nanoscale particles in tissue engineering, gas transport, nanomedicine, and immunological factors, the canvas widens to show a comprehensive analysis of the body of current work. This chapter lays out the background, highlighting key areas of unmet research need and developing goals to drive our search for solutions.

Objectives of this Dissertation:

Objective I: Synthesis of biopolymeric nanoparticles for enhanced skin regeneration.

Objective II: Wound healing activity potentiation of PNAG NPs for enhanced skin regeneration.

Objective III: Evaluation of biological activity of metal oxide antimicrobial nanoparticles for complex and bacteria infected wounds.

Chapter 2: Materials and Experimental Procedures

This chapter delves into the fundamental components of our study: the substances and procedures that gave rise to the unique biopolymeric nanoparticles. We show off the painstaking workmanship that goes into every step of our research process, from synthesis to characterisation, drug loading to release capabilities, and in vitro to in vivo investigations. Nitric oxide (NO) delivery research is already underway, providing a bright light for improved skin regeneration.

Chapter 3: Results and Discussions

Our laborious experiments are indicated by the complex brushstrokes in Chapter 3. A component of our research goals is revealed in each subchapter, ranging from the creation and testing of PNAG NPs for skin regeneration to the enhancement of wound healing with NO and the thorough biological activity analysis of metal oxides. A colourful display

of scientific investigation is created by the figures and discoveries that dance over these pages.

Chapter 4: The Culmination - Summary, Conclusions, and Future Scope

By the time this dissertation comes to an end, the synthesized PNAG NPs become the heroes in the story of wound healing. Their potential for topical applications in regenerative nanomedicine is indicated by their capacity to promote angiogenesis, decrease inflammation, and accelerate healing rates *in vivo*. The partnership with NO, included in SP NPs, demonstrates synergistic benefits that outperform conventional therapies, opening the door for adaptable formulations that may be used in a variety of wound types.

Our adventure doesn't finish here, though. Metal oxides' biological activities reveal them as possible partners in the battle against microbial contaminated wound and diseases. These nanoparticles hold great potential for medicinal applications, cell compatibility, and antibacterial activities, opening up new research directions.

The Future Awaits

This dissertation serves as both a capstone and an inspiration for future endeavors. Researchers are encouraged to push the frontiers further by means of sophisticated delivery technologies, clinical trials, optimization tactics, and thorough mechanistic investigations. Successful regenerative nanomedicine incorporation into clinical practice requires smart technology integration, teamwork, and public awareness campaigns.

We establish not only a basis in these pages, but also a vision that inspires, presents opportunities, and drives the search for revolutionary breakthroughs in wound care and therapeutic technology. This is a call to action for the scientific community to work together to shape the direction of regenerative nanomedicine, not simply a dissertation. The trip never ends, and there are countless opportunities.

Table of Contents

<i>Certificate</i>	ii
<i>Declaration by the Candidate & Certificate by the Supervisor</i>	iii
<i>Copyright Transfer Certificate</i>	iv
<i>Acknowledgement</i>	v
<i>Abstract</i>	vi-vii
<i>Table of Contents</i>	viii-xii
<i>List of figures</i>	xiii-xix
<i>List of Tables</i>	xx
<i>List of Abbreviations</i>	xxi-xxiii
<i>Preface</i>	xxiv-xxv
CHAPTER 1: INTRODUCTION AND BACKGROUND	1
1.1 INTRODUCTION	1
1.2 ORIGINS AND CATEGORIES OF WOUNDS	2
1.3 WOUND HEALING PROCESS	5
1.3.1 Haemostasis Phase	6
1.3.2 Inflammatory Phase	7
1.3.3 Cell Proliferation and Migration	8
1.3.4 Remodelling of Tissues	9
1.4 MATERIALS FOR WOUND DRESSING	10
1.4.1 Nanoparticles and Their Application in Wound Healing	11
1.4.2 Nanoparticles Employed in Wound Healing Therapy	21
1.5 EXPLORING NANOTHERAPEUTICS: ADVANCING WOUND HEALING INNOVATIONS	23
1.6 GASEOUS INNOVATIONS: PIONEERING WOUND HEALING STRATEGIES	26
1.7 NITRIC OXIDE	29
1.7.1 NO for Vasodilation and Increased Blood Flow	30
1.7.2 NO for Anti-Inflammatory Properties	30
1.7.3 NO for Angiogenesis Stimulation	30
1.7.4 NO for Collagen Synthesis and Tissue Remodeling	31
1.7.5 Antimicrobial Effects	31

1.7.6	Cell Proliferation and Migration	31
1.7.7	NO for the Regulation of Matrix Metalloproteinases (MMPs)	31
1.7.8	NO for the Neurotransmitter Function	31
1.7.9	Ischemia-Reperfusion Injury Protection	32
1.7.10	Low Toxicity and Versatility of NO Delivery	32
1.7.11	Synergistic Effects of NO with Other Growth Factors	32
1.7.12	Modulation of Oxidative Stress by NO	33
1.7.13	Therapeutic Potential of NO in Chronic Wounds	33
1.7.14	Clinical Evidence and Established Therapies Using NO	33
1.8	MOTIVATION FOR DEVELOPMENT OF ADVANCED NANOTHERAPEUTICS AS REGENERATIVE NANOMEDICINE	34
1.8.1	Medical Need and Social Impact	34
1.8.2	Economic Considerations	35
1.8.3	Scientific Advancement	35
1.8.4	Ethical Considerations	35
1.9	STATEMENT OF PROBLEM (EXISTING CHALLENGES AND RESEARCH GAPS)	36
1.9.1	Existing Challenges	36
1.9.2	Research Gap	37
1.10	OBJECTIVES	41
1.10.1	Objective 1	41
1.10.2	Objective 2	42
1.10.3	Objective 3	42
1.11	REFERENCES	43
	CHAPTER 2: MATERIALS AND METHODOLOGIES	61
2.1	MATERIALS	61
2.2	METHODOLOGIES	62
2.2.1	Synthesis and Preparation of PNAG and SP NPs	62
2.2.2	Synthesis of Metal Oxides Nanoparticles	63
2.3	CHARACTERIZATION	65

Table of Contents

2.3.1	Chemical Group Confirmation	65
2.3.2	Fourier Transform Infrared (FTIR)	65
2.3.3	Nuclear Magnetic Resonance (NMR)	65
2.3.4	Transmission Electron Microscopy (TEM)	66
2.3.5	Scanning Electron Microscopy (SEM)	66
2.3.6	Dynamic Laser Scattering (DLS) and Zeta Potential Estimation	67
2.3.7	X-ray Diffraction (XRD)	67
2.4	<i>IN VITRO</i> CELL CULTURE STUDIES	67
2.4.1	Cell Viability: MTT Assay	67
2.4.2	Cell Proliferation and Migration: Scratch Wound Assay	69
2.4.3	Live/dead Assay	70
2.5	HAEMOCOMPATIBILITY STUDY	70
2.5.1	Haemolysis Assay	69
2.5.2	Blood Coagulation Study	71
2.6	NITRIC OXIDE LOADING AND RELEASE DETERMINATION	72
2.6.1	Loading of Gas Releasing Molecules in to PNAG NPs	72
2.6.2	Entrapment Efficiency (EE, %) and Loading Capacity (LC, %)	72
2.6.3	Determination of NO Content and NO Release Profile	72
2.7	NANOFORMULATION DEVELOPMENT AND EVALUATION	73
2.7.1	Preparation of Nanoformulation and Qualitative Evaluation	73
2.7.2	Physicochemical Evaluation of SP Nanoformulation	74
2.8	BIOLOGICAL EVALUATION OF NANOFORMULATION	77
2.8.1	Angiogenesis: Chicken Embryo Angiogenesis Assay (CAM assay)	77
2.8.2	Animal Protocol and Ethics	78
2.8.3	Dermal Irritation Study	79
2.8.4	<i>In vivo</i> Wound Healing Study Protocol	80

2.8.5	Histological Analysis	81
2.8.6	Immunochemical Analysis	81
2.8.7	Semi-Quantitative Reverse Transcription and Polymerase Chain Reaction (sqRT-PCR)	82
2.9	STATISTICAL ANALYSIS	83
2.10	REFERENCES	83
CHAPTER 3: RESULTS AND DISCUSSIONS		85
CHAPTER 3: PART I		87
3.1	Development and Evaluation of Biopolymeric PNAG NPs for Advanced Skin Regeneration in Wound Healing	87
3.1.1	ABSTRACT	87
3.1.2	INTRODUCTION	88
3.1.3	EXPRIMENTAL	91
3.1.4	RESULTS	93
3.1.5	DISCUSSION	118
3.1.6	CONCLUSIONS	123
3.1.7	REFERENCES	124
CHAPTER 3: PART II		129
3.2	Potentialion of Wound Healing Activity of PNAG NPs With Nitric Oxide for Enhanced Skin Regeneration	129
3.2.1	ABSTRACT	129
3.2.2	INTRODUCTION	130
3.2.3	EXPRIMENTATION	133
3.2.4	RESULTS	135
3.2.5	DISCUSSION	163
3.2.6	CONCLUSIONS	169
3.2.7	REFERENCES	170
CHAPTER 3: PART III		177
3.3	Comprehensive Biological Activity Assessment of Metal Oxides in Wound Healing	177
3.3.1	ABSTRACT	177
3.3.2	INTRODUCTION	179
3.3.3	EXPRIMENTAL	180

Table of Contents

3.3.4	RESULTS	181
3.3.5	DISCUSSION	203
3.3.6	CONCLUSIONS	204
3.3.7	REFERENCES	205
CHAPTER 4:	SUMMARY, CONCLUSIONS AND FUTURE	207
	PROSPECTS	
4.1	Summary and Conclusion	207
4.2	Future Scope of Present Work	212

Appendix

MALDI-TOF
Ethical Approval
Similarity Report
List of Publications
Resume

Abstract

Advanced wound healing research addresses severe clinical issues by developing novel treatments to optimize the process and reduce vulnerability to fatal microbial infections. Effective wound healing requires proficient orchestration between immune and biological systems. This study aimed to formulate poly(N-acryloyl glycine) nanoparticles (PNAG NPs) to enhance skin restoration. PNAG NPs, about c.a. 35 nm in diameter, were synthesized using mini-emulsion radical polymerization and incorporated into an ointment. TNF- α and IL6 levels in the PNAG nanoformulation treated group shifted from 4.10 ± 3.18 to 5.17 ± 3.27 pg mL⁻¹ and 11.93 ± 2.34 pg mL⁻¹ to 10.33 ± 3.31 pg mL⁻¹, respectively, indicating reduced inflammation while IGF-1 levels increased from 25.41 ± 13.56 ng mL⁻¹ to 64.22 ± 16.93 ng mL⁻¹, correlating with enhanced angiogenesis and improved wound healing. PNAG NPs also facilitated coordinated cell proliferation, migration, anti-inflammatory responses, and simultaneous skin tissue regeneration without external synergistic factors. The cytocompatible and hemocompatible PNAG nanoformulation demonstrated 31% higher wound healing efficiency compared to the control group *in vivo*.

Further, the regenerative potential of PNAG NPs was potentiated by harnessing the regenerative power of Nitric Oxide (NO) by the loading of NO donor [Sodium nitroprusside (SNP): a well-known NO donor]. The SNP loaded PNAG NPs are termed as SP NPs and can release NO in sustained manner for more than 24 hours, crucial for wound healing. SP NPs promoted significant proliferation (~300%) and migration of L929 cells. Haemocompatibility studies in isolated rat blood components confirmed the safety of SP NPs. The SP nanoformulation showed excellent angiogenic activity, non-toxicity, and can closed wounds significantly faster ($99.2 \pm 1.0\%$) within 13.23 days than the control group ($45.5 \pm 3.8\%$) *in vivo*, demonstrating its clinical potential for tissue regeneration.

Further, the metal oxide (ZnO, ZnO-CuO, ZnO-Ag₂O, ZnO-SnO₂) antimicrobial nanoparticles had been synthesized by keeping in mind that these will be applied in the treatment of complex infected skin wounds. Given the threat of antimicrobial resistance, nanoparticles were utilized for their properties. ZnO and its metal composites, including ZnO-CuO, ZnO-Ag₂O/Ag, and ZnO-SnO₂ NPs, showed excellent antimicrobial properties against various microbes. These nanoparticles have their particle size below

10 nm, demonstrated mesoporous structures and nanocrystallinity, confirming their antibacterial activity in a dose- and time-dependent manner. Hemocompatibility assessments revealed low haemolysis, with ZnO-CuO exhibiting the lowest haemolytic nature. Cytocompatibility studies showed compatibility with L929 cells, particularly for ZnO and ZnO-SnO₂ nanocomposites. Cell migration and proliferation evaluations in scratch wound healing model highlighted the superior performance of ZnO-SnO₂, followed by ZnO, ZnO-Ag₂O, and ZnO-CuO. ZnO-CuO nanocomposite showed the highest angiogenic potential evaluated *in ovo*, suggesting its potential application in tissue regeneration through wound healing. In our work PNAG NPs demonstrated efficacy in coordination of cellular response, anti-inflammatory actions, and angiogenesis which collectively accelerating the skin regeneration. Further, sustained NO release via SP NPs exhibited remarkable proliferation and migration capabilities, proving their clinical potential and metal oxide nanocomposites, especially ZnO-CuO, showed promising antimicrobial, hemocompatible, and cell-compatible properties, making them valuable for therapeutic wound healing applications.